

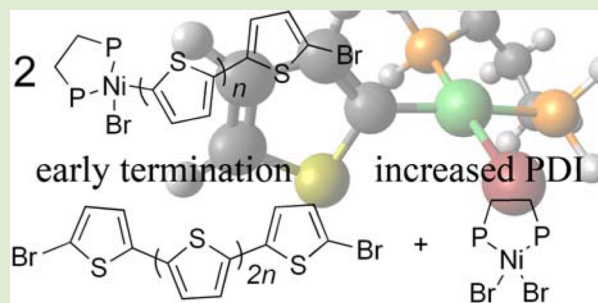
On the Role of Disproportionation Energy in Kumada Catalyst-Transfer Polycondensation

Jenna A. Bilbrey,^{†,§} S. Kyle Sontag,[†] N. Eric Huddleston,[†] Wesley D. Allen,^{*,†,§} and Jason Locklin^{*,†,‡}

[†]Department of Chemistry, [‡]College of Engineering, Center for Nanoscale Science and Engineering, and [§]Center for Computational Chemistry, University of Georgia, Athens, Georgia 30602, United States

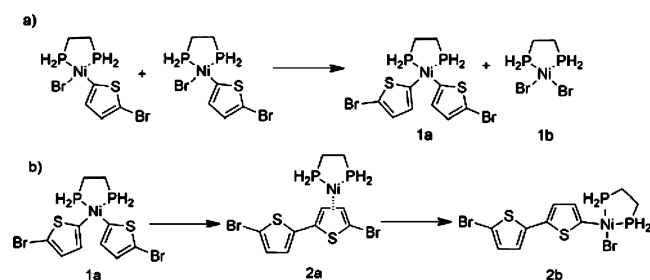
Supporting Information

ABSTRACT: Kumada catalyst-transfer polycondensation (KCTP) is an effective method for the controlled polymerization of conjugated polymers. Nevertheless, side reactions leading to early termination and unwanted chain coupling cause deviations from the target molecular weight, along with increasing polydispersity and end group variation. The departure from the KCTP cycle stems from a disproportionation reaction that leads to experimentally observed side products. The disproportionation energies for a series of nickel-based initiators containing bidentate phosphino attendant ligands were computed using density functional theory at the B3LYP/DZP level. The initiator was found to be less favorable toward disproportionation by 0.5 kcal mol⁻¹ when ligated by 1,3-bis(diphenylphosphino)propane (dppp) rather than 1,2-bis(diphenylphosphino)ethane (dppe). Trends in disproportionation energy (E_{disp}) with a variety of bidentate phosphine ligands match experimental observations of decreased polymerization control. Theoretical E_{disp} values can thus be used to predict the likelihood of disproportionation in cross-coupling reactions and, therefore, aid in catalyst design.



Kumada catalyst-transfer polycondensation (KCTP) has been shown to undergo a chain-growth polymerization mechanism affording polymers with controlled molecular weight, narrow polydispersity (PDI), and uniform chain-ends.^{1–3} KCTP, which employs a nickel-based initiating complex, deviates from living polymerization due to premature termination, as evidenced by both high and low molecular weight components in the reaction mixture displaying nonuniform chain-ends.^{4,5} A major contributor to the loss of living character stems from a disproportionation reaction in which two (aryl)Ni(II)–Br complexes exchange ligands, forming an (aryl)₂Ni(II) intermediate along with Ni(II)Br₂ (Scheme 1a). After subsequent reductive elimination and carbon–carbon coupling of the activated complex (1a), the nickel(0) remains η -bound to the biaryl product (2a) before undergoing intramolecular insertion into the carbon–halogen bond (2b) (Scheme 1b).⁶

Scheme 1. Disproportionation Reaction of Ni(dhpe)ThBr



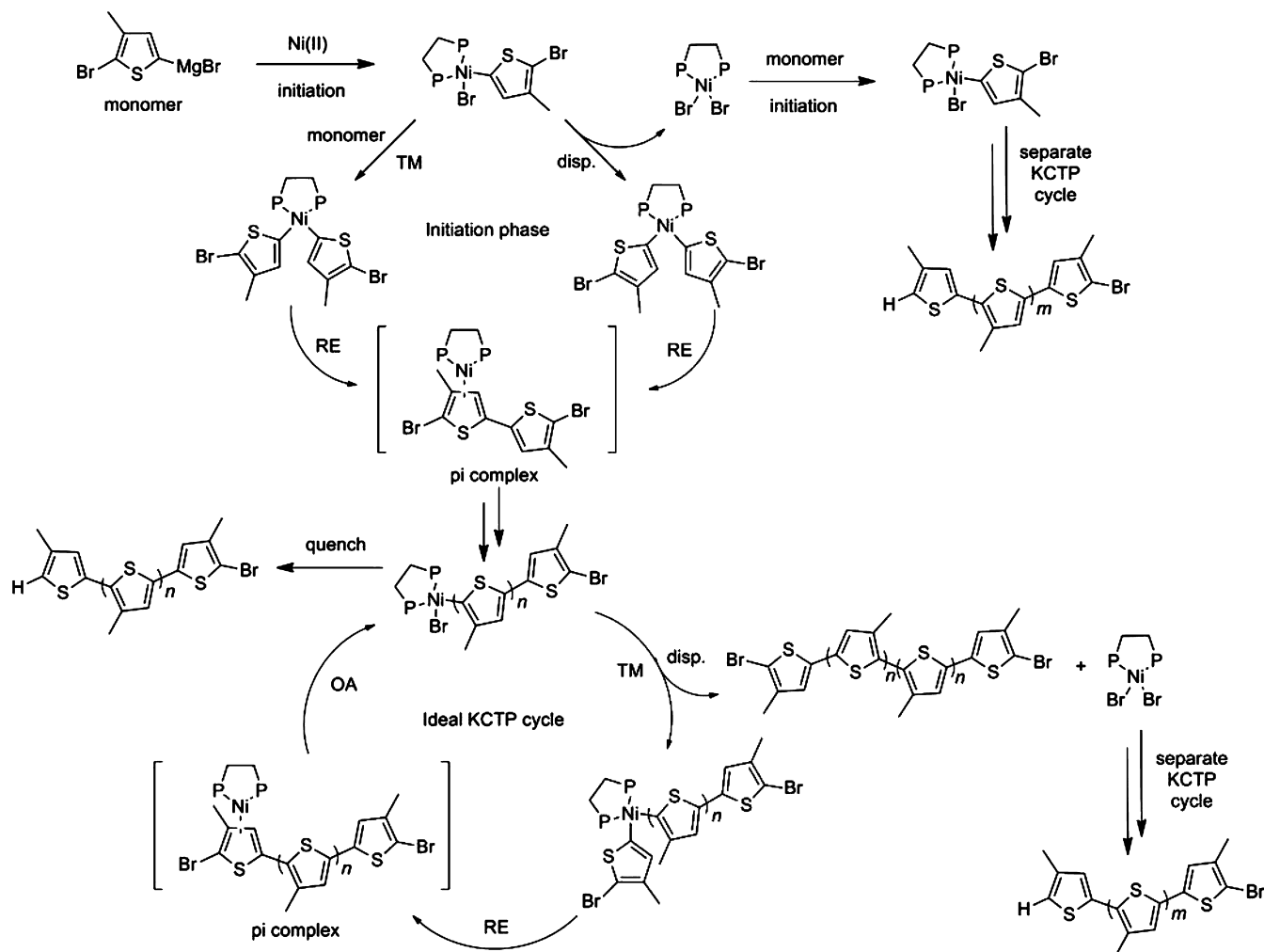
In KCTP, the desired polymerization route involves a Grignard AB-type monomer, which undergoes a repeated cycle of transmetalation (TM), reductive elimination (RE), and oxidative addition (OA) (Scheme 2). After the polymerization is quenched by aqueous acid, resulting chains are of uniform length and contain H/Br end groups. In addition to the ideal cycle, disproportionation can occur whenever an (aryl)Ni(II)Br is present (i.e., prior to initiation and transmetalation). During the initiation phase, two initiator complexes can exchange ligands through disproportionation, releasing free Ni(II)Br₂ into solution, which has been spectroscopically observed during polymerization.⁵ The Ni(II)Br₂ is reactivated by a double transmetalation reaction with excess monomer and taken through a separate KCTP cycle, which results in an increased polydispersity due to varying chain lengths. Disproportionation can also occur after the initiation phase but prior to transmetalation in the ideal cycle, yielding polymers of double molecular weight as well as Ni(II)Br₂. The Ni(II)Br₂ is released into solution, reactivated, and undergoes another separate KCTP cycle to further increase polydispersity.

Disproportionation is often seen in the Kumada coupling of small-molecule biaryls, which is the parent reaction of KCTP.^{7–11} Due to the nature of polymerizations, however, the direct observation of disproportionation in situ is difficult. For this reason, we have modeled disproportionation through a

Received: June 11, 2012

Accepted: July 13, 2012

Published: July 20, 2012

Scheme 2. General Reaction Cycle for KCTP^a

^aDisproportionation is the cause of increased polydispersity, resulting in chains with H/Br end groups and coupled-chains with Br/Br end groups. TM = transmetalation, RE = reductive elimination, OA = oxidative addition, and disp = disproportionation.

series of computational experiments. The tendency for an initiating complex to disproportionate can be quantified by the relative disproportionation energy (E_{disp}), which is a thermodynamic quantity. A positive value represents lower energy in the reactants resulting in a decreased likelihood of disproportionation. Conversely, negative energies correspond to an increased likelihood of disproportionation.

Because the living characteristics of the polymerization are known to differ according to the choice of attendant ligand, we have examined a series of commonly employed bidentate phosphino ligands differing in either the carbon spacer or phosphorus substituent (Figure 1), which influence the bite and cone angle parameters of the catalysts.^{4,5} In this report, we have observed that the polymerization character is highly influenced

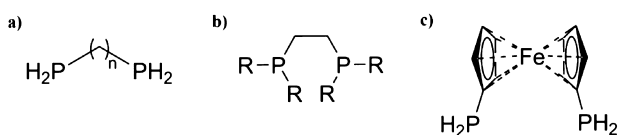


Figure 1. Ligands studied in this report, abbreviated as follows: (a) $n = 2$: dhpe, $n = 3$: dhpp, $n = 4$: dhpb, (b) $R = \text{H}$: dhpe, $R = \text{methyl}$: dmpe, $R = \text{ethyl}$: depe, $R = \text{phenyl}$: dppe, (c) dhpf.

by the ability of the initiator to undergo disproportionation and not by trends in either bite angle or cone angle. Deviations in polymerization control can be inferred by the polydispersity index (PDI) and resultant end groups. Herein, we match trends in computed disproportionation energies to PDIs from several literature reports^{4,5} and conclude that the loss of polymerization control follows the trend of increased disproportionation.

The bite angle involving the attendant ligand (P–Ni–P angle here) has been speculated to strongly influence polymerization control.^{4,12} Adding units to the carbon spacer of the ligand has the effect of increasing the bite angle about the nickel center. Once the spacer exceeds three carbons, polymerization becomes less controlled and undergoes intermolecular catalyst transfer, resulting in increased polydispersity and varying end groups.⁴

In the investigation of bite angle, hydrogen atoms were substituted for phenyl groups on the phosphino ligands to keep steric crowding at a minimum and improve computational efficiency. This is a common simplification shown to be valid in previous reports.^{13,14} The order of experimentally averaged P–Ni–P bite angles (obtained from a large number of X-ray crystallographic structures from the Cambridge Structural

Database) is consistent with the structures computed in this report for various spacers: ethyl < propyl < ferrocenyl < butyl.¹⁵

To examine the role of bite angle, disproportionation energies were computed for a series of initiating species differing only in backbone of the attendant ligand (Table 1).

Table 1. Comparison of Ni(II) Initiators Differing in Attendant Ligand Bite Angle

attendant ligand	E_{disp}^a	mean X-ray bite angle ^b	computed bite angle ^c	PDI ^d P3HT	PDI ^d PPP
dhpe	0.0	85.0	88.3	1.50	2.66
dhpp	6.2	91.1	97.4	1.12	1.74
dhpf	1.0	95.6	101.5	1.83	2.40
dhpB	-4.3	97.7	104.4	2.40	

^aRelative values given in kcal mol⁻¹. ^bAveraged crystallographic bite angles for an array of phenyl substituted species.¹⁵ ^cFor isolated complexes at the B3LYP/DZP level of theory. ^dReported polydispersities of poly(3-hexylthiophene) (P3HT) and poly(2,5-dihexyloxyphenylene) (PPP) synthesized from catalysts with phenyl substituents on the phosphorus atoms.⁴

Thiophene (Th) units were used as the aryl species. Reported E_{disp} energies are referenced to Ni(dhpe)BrTh to single out the trends. Total electronic energies are given in the Supporting Information (ESI, Table 1).

The relative disproportionation energies of 1,2-bis(dihydrophosphino)ethane (dhpe; 0.0), 1,3-bis(dihydrophosphino)propane (dhpp; 6.2), 1,4-bis(dihydrophosphino)butane (dhpB; -4.3), and 1,1'-bis(dihydrophosphino)ferrocene (dhpf; 1.0) predict that the trend in polymerization control is dhpB < dhpe < dhpf < dhpp. This is in sharp contrast to the order of bite angle: dhpe < dhpp < dhpf < dhpB. Comparing previous PDI measurements for poly(3-hexylthiophene) (P3HT) by Miyakoshi et al.⁴ which indicate a trend in control of dhpB < dhpf < dhpe < dhpp, it is clear that the experimental trend is best matched by our predictions based on disproportionation energies.

A discrepancy does exist between the reduced control in polymerization of P3HT with the ferrocenyl-based ligand and the computed positive disproportionation energy. A primary difference between dhpf and the other ligands studied is the different electronic properties associated with the ferrocenyl backbone compared to a simple alkyl spacer. Using the ferrocenyl ligand, Miyakoshi et al.⁴ synthesized low molecular weight polymer with high polydispersity and diverse end groups. This result is in contrast to what is expected based on our disproportionation energy computations. When LiCl was added to the polymerization in an effort to increase the rate of transmetalation to bypass side reactions such as disproportionation, a polymer with higher molecular weight and smaller PDI was achieved when dppe or dppp was the attendant ligand. The LiCl addition did not increase polymerization control when dppf was the attendant ligand; a polymer of low molecular weight, high PDI (2.78), and varying end groups resulted. These observations indicate that an alternative reaction which does not compete with transmetalation is the cause of lessened control. The reaction rate of oxidative addition has been shown to be slow for dppf.^{16,17} Slow oxidative addition may allow for dissociation of Ni(0) from the growing chain resulting in uncontrolled polymerization.

Relative disproportionation energies were also computed for complexes with 3-methylthiophene rather than thiophene as the aryl group. The same trend is followed with values of 0.4

kcal mol⁻¹ for dhpe, 6.4 kcal mol⁻¹ for dhpp, -4.6 kcal mol⁻¹ for dhpB, and 1.5 kcal mol⁻¹ for dhpf. All values are in reference to complexes ligated by dhpe with thiophene as the aryl group. In most of the cases, the addition of an ortho substituent lessens disproportionation reactions, as E_{disp} is slightly raised for dhpe, dhpp, and dhpf. For dhpB, however, a greater amount of disproportionation is expected. An increase in side chain length was not expected to change trends in thermodynamics of the system, and substituting a hexyl chain did not affect the trend for disproportionation (ESI Table 1). In fact, when dhpe was the attendant ligand, the disproportionation energy increased by 2.4 kcal mol⁻¹ with a hexyl substituent relative to unsubstituted thiophene; therefore disproportionation is less likely with the hexyl substituent present.

Interestingly, the polymerization of poly(2,5-dihexyloxybenzene) (PPP)⁴ also broadly follows the trend of higher PDI with decreasing E_{disp} found with thiophene as the aryl group. Therefore, the disproportionation trends seem to be based on attendant ligand characteristics more so than the electron donating/withdrawing abilities of the monomer itself.

Another geometric feature of the initiating complex is steric crowding of the nickel center, which can be approximately gauged by the cone angle occupied by the ligand molecules.¹⁸ Following Lanni et al.,⁵ we have studied a set of ligands with similar bite angles ranging from 87.3° to 92.2° and widely varying cone angles (Table 2). All reported E_{disp} energies are in reference to Ni(dppe)BrTh. Total electronic energies can be found in ESI Table 1.

Table 2. Comparison of Ni(II) Initiators Differing in Attendant Ligand Cone Angle

attendant ligand	E_{disp}^a	bite angle ^b	cone angle ^c	PDI ^d PPP	PDI ^d P3HT	PDI ^e P3HT
dmpe	1.2	88.3	156	1.51		
depe	-5.6	87.4	176	2.12	2.26	
dppe	0.0	87.3	178	2.42 ^f	2.29 ^f	1.50
dppp	0.5	92.2	183	3.59 ^f	1.77 ^f	1.12

^aRelative values given in kcal mol⁻¹. ^bCalculated from optimized B3LYP/DZP geometries. ^cFrom ref 18. ^dReported polydispersities of poly(2,5-dihexyloxyphenylene)(PPP) and poly(3-hexylthiophene)-(P3HT) from ref 5. ^eReported polydispersities of poly(2,5-dihexyloxyphenylene)(PPP) and poly(3-hexylthiophene)(P3HT) from ref 4. ^fPolymerization conditions were not optimized.

As found for the bite angle, trends in polymerization characteristics do not follow that of increasing or decreasing cone angle, which are 156°, 176°, 178°, and 183° for 1,2-bis(dimethylphosphino)ethane (dmpe), 1,2-bis(diethylphosphino)ethane (depe), 1,2-bis(diphenylphosphino)ethane (dppe), and 1,3-bis(diphenylphosphino)propane (dppp), respectively, as reported in a survey of crystallographic structures from the Cambridge Structural Database.¹⁸ Disproportionation energies show depe to have the highest tendency toward disproportionation with a value of -5.6 kcal mol⁻¹. The dppp ligand, with a value of 0.5 kcal mol⁻¹ is slightly less likely than dppe to undergo disproportionation. Surprisingly, dmpe has a relatively high disproportionation energy of 1.2 kcal mol⁻¹ and as such should not undergo disproportionation as readily. This forms the predicted trend in polymerization control of depe < dppe < dppp < dmpe.

Recently, Lanni et al.⁵ investigated ligand-based steric effects using the four ligands in Table 2 to polymerize both 4-bromo-

2,5-bis(hexyloxy)phenylmagnesium chloride and 2-bromo-3-hexyl-5-thienylmagnesium chloride. Although correlations from disproportionation energy anticipate *dmpe* to minimize disproportionation, it is kinetically unstable and decomposes in solution under the conditions of these polymerizations (60 °C).⁵ In the polymerization of P3HT using *depe* as the attendant ligand, Lanni et al.⁵ observed a broad polydispersity index (2.26). They attributed this to slow initiation (compared to *dppp* and *dppe*), which the authors also observed when investigating the initiation rate of the phenylene monomer. With the two competing reactions, the slowing of this key step (initiation) could increase the likelihood of disproportionation. Disproportionation at the initiation stage only increases polydispersity by the formation of Ni(II)Br₂, which initiates a new polymerization cycle and does not change the nature of resultant chain ends (Scheme 2). In fact, with the use of *depe*, free Ni(II)Br₂ was observed by ³¹P NMR during polymerization, which the authors ascribed to disproportionation.⁵

Following the trend in disproportionation energy, polymerization with *depe* as the attendant ligand should exhibit less control than polymerization with *dppe* or *dppp*. In the aforementioned study, however, polydispersities for *dppe* and *dppp* were higher than expected for a controlled chain-growth polymerization. This is likely due to high reaction temperatures as all polymerizations were carried out at 60 °C for a direct comparison of polymerization rate-determining steps. The increased reaction temperature was used to overcome the slow initiation present with *depe*. At reduced polymerization temperatures (25 °C), Miyakoshi et al.⁴ observed a low PDI in the polymerization of P3HT for both *dppe* (1.50) and *dppp* (1.12), consistent with the trend in disproportionation energies. As such, *dppp* is shown to minimize disproportionation, but the reaction is not completely suppressed. Smeets et al.¹⁹ observed 10% of P3HT synthesized with initiator ligated by *dppp* to contain various unexpected end groups (Br/Br, H/H, etc.), which shows that disproportionation as well as other side reactions still occur.

Excluding *dmpe* due to lack of stability, experiments have shown *dppp* to be the best performing ligand for KCTP followed by *dppe*, while polymerizations with *depe* display a high polydispersity.^{4,19} This matches our predicted trend in disproportionation energy of *depe* < *dppe* < *dppp*. Although *depe* and *dppe* have similar cone angles (~177°), *dppe* has been shown to have greater polymerization control and a decreased tendency toward disproportionation.

An alternative factor that potentially causes loss of polymerization control is Ni(0) diffusion after the reductive elimination step, which results in early termination as well as unwanted reinitiation. While the exact mechanism is still unclear, Kiriy et al. have convincingly argued that a single nickel complex polymerizes one chain.²⁰ Early mechanistic work came from the groups of McCullough and Yokozawa. McCullough et al.²¹ stated that the nickel complex and growing chain generate an associated pair in which Ni(0) does not diffuse away. Following that, Yokozawa et al.²² suggested intramolecular transfer of the nickel complex into the terminal C–Br bond of the polymer, which implies some sort of association. Intramolecular transfer was demonstrated by examination of the initiator (aryl)Ni(II)Br formed in situ during the polymerization process.⁴ Two thiophene units were coupled together to analyze end groups of the newly formed bithiophene. Polymer with H/Br end groups indicate intramolecular transfer, while Br/Br end groups indicate Ni(0) diffusion. Even at extremely high concentrations

of catalyst (50 mol %), only bithiophene with Br/H end groups were observed, meaning that nickel diffusion does not occur.

Additionally, experimental and computational work has shown that Ni(0) can remain η -bound with a conjugated ring and “walk” along the π -framework until insertion into a C–Br bond is possible.²³ Komber et al.²⁴ have recently observed disproportionated products concomitant with strong Ni(0) binding and decreased ring-walking ability due to electron-deficient aromatic monomer units. These arguments strongly suggest that free nickel diffusion after the reductive elimination step is unlikely. Therefore, disproportionation must be a major termination pathway that accounts for large molecular weight deviations and end group discrepancy.

A lone report by Achord and Rawlins²⁵ argues in favor of nickel diffusion, but with a high rate of reassociation. A key argument in their case was the observation of Br/Br end groups, which do not result from the proposed KCTP chain-growth mechanism, and which the authors claim is due to diffusion of free Ni(0). The authors did not consider other possible modes of termination or reinitiation, such as disproportionation, which can form a polymer with Br/Br end groups (Scheme 2). Additionally, the authors observed that an increase in reaction time at high conversion leads to an increase in the percentage of undesired, double molecular weight Br/Br terminated polymer. We argue that the extended time period allowed for disproportionation as the monomer concentration decreased, and thus nickel complexes had an increased probability of reacting with one another to undergo disproportionation.

In addition to Ni(0) dissociation, it is possible that magnesium halogen exchange can increase polydispersity.^{19,26} In this reaction a bromine atom at the terminal end of the polymer chain exchanges with the magnesium chloride group of the monomer. This exchange places the Grignard reagent at the end of the chain, which can transmetalate with another (aryl)Ni(II)Br, causing further polymerization from both ends. Quenching results in H/H end groups which are distinctive from disproportionation and Ni(0) dissociation since both reactions only form polymer with H/Br and Br/Br end groups. Two studies have observed P3HT with H/H end groups and attributed this to a combination of magnesium-halogen exchange reactions and impure monomer.^{19,28}

This report has indicated that loss of polymerization control in nickel-catalyzed cross-coupling reactions is not solely the effect of ligand geometry but stems from a competing termination reaction: disproportionation. This process explains the decrease in control observed by some initiating species and is accomplished without nickel diffusion from the polymer chain after the reductive elimination step. If disproportionation happens late in the polymerization, the polydispersity index can be directly compared to the amount of unwanted side reactions by the appearance of a shoulder of double molecular weight in the gel permeation chromatogram.^{4,5} PDI as well as analysis of end groups can be compared to theoretically computed disproportionation energies to provide trends arising from different ligands.

Scheme 2 shows the two stages during the polymerization cycle where disproportionation is a competing reaction: initiation and transmetalation. Disproportionation at the initiation stage releases free Ni(II)Br₂ into solution, which is reactivated by a double transmetalation reaction with two equivalents of monomer to start a separate polymerization cycle. Likewise, disproportionation in lieu of the trans-

metalation step results in chain-coupling to form higher molecular weight chains with Br/Br end groups. Free Ni(II)Br₂ is formed as well, which is once again reactivated to undergo further KCTP cycles, increasing polydispersity.

Numerous experiments have confirmed improved control of KCTP by use of lithium chloride, which speeds both initiation and transmetalation steps.^{5,27,28} As the rate of precatalyst initiation is increased, subsequent competing reaction pathways are outpaced, resulting in polymers of highly uniform molecular weight.²⁹ These results suggest avoidance of the disproportionation pathway by accelerating the initiation step. Similarly, the rate of transmetalation is increased by forming a highly active “turbo-Grignard”.³⁰ Reactions with turbo-Grignard allow transmetalation to proceed at a faster rate than disproportionation, removing the bimodal molecular weight distribution.

Miyakoshi et al.⁴ observed a narrowing of molecular weight distribution and the disappearance of a high molecular weight shoulder at reduced reaction temperatures. The decreasing temperature must slow the rate of disproportionation such that the reaction is no longer competitive with the rate of transmetalation. This result, in conjunction with our computed trends, shows that polymerization control is strongly influenced by disproportionation energy, more so than ligand geometry. Computed E_{disp} values can be used to predict the presence of disproportionation in cross-coupling reactions and, therefore, aid in catalyst design. Further computational studies are currently underway to investigate additional details of other transition-metal mediated cross-coupling polymerizations.

THEORETICAL METHODS

The energetics of all species were computed with zero-point vibrational energy (ZPE) corrections using density functional theory with the QChem3.2 package.³¹ Reported values were computed with the B3LYP functional,^{32,33} which has been shown to properly model organometallic transition metal complexes.^{34–37} Three other functionals, M06, B97, and PBE, were also shown to give matching trends (ESI Table 2).^{38,39} Benchmarking our DFT methods with coupled-cluster singles and doubles (CCSD)⁴⁰ computations on a small model system shows B3LYP to give disproportionation energies very close to rigorous electron-correlated values (ESI Table 2). For all atoms except halogens and transition metals, the Dunning standard double- ζ contraction of Huzinaga primitive sets was used in accord with a previous work.^{41,42} Halogens were treated using effective core potentials of the Stuttgart-Bonn type with complementary basis sets.⁴³ Following Schaefer et al.,^{44,45} nickel and iron employed the Wachters primitive sets in a loosely contracted DZP fashion, augmented with two sets of p and one set of d functions, giving the total contraction scheme (14s11p6d/10s8p3d). All complexes were confirmed to be local minima by the absence of imaginary vibrational frequencies. A radial, angular (75, 302) grid was accurate enough for most complexes; in some cases a (99, 590) grid was used to eliminate small imaginary frequencies. Several stable geometric orientations are possible for the phenyl moieties; we have used the lowest energy conformation described in previous reports.⁴⁶

ASSOCIATED CONTENT

Supporting Information

Total electronic energies along with optimized Cartesian coordinates of all stationary points, comparison and benchmarking of functionals, and out-of-plane angles for all reactants. This material is available free of charge via the Internet at <http://pubs.acs.org>.

AUTHOR INFORMATION

Corresponding Author

*E-mail: wdallen@uga.edu (W.D.A.); jlocklin@uga.edu (J.L.).

Notes

The authors declare no competing financial interest.

ACKNOWLEDGMENTS

This work was supported by the Donors of the American Chemical Society Petroleum Research Fund (Grant 48917-DNI7) and the National Science Foundation (CHE 1058631 and DMR 0953112).

REFERENCES

- (1) Sheina, E. E.; Liu, J.; Iovu, M. C.; Laird, D. W.; McCullough, R. D. *Macromolecules* **2004**, *37*, 3526–3528.
- (2) Yokoyama, A.; Miyakoshi, R.; Yokozawa, T. *Macromolecules* **2004**, *37*, 1169–1171.
- (3) Beryozkina, T.; Senkovskyy, V.; Kaul, E.; Kiriy, A. *Macromolecules* **2008**, *41*, 7817–7823.
- (4) Miyakoshi, R.; Yokoyama, A.; Yokozawa, T. *J. Polym. Sci., Part A: Polym. Chem.* **2008**, *46*, 753–765.
- (5) Lanni, E. L.; Locke, J. R.; Gleave, C. M.; McNeil, A. J. *Macromolecules* **2011**, *44*, 5136–5145.
- (6) Zenkina, O. V.; Karton, A.; Freeman, D.; Shimon, L. J. W.; Martin, J. M. L.; van der Boom, M. E. *Inorg. Chem.* **2008**, *47*, 5114–5121.
- (7) Negishi, E.; King, A. O.; Okukado, N. *J. Org. Chem.* **1977**, *42*, 1821–1823.
- (8) Sainsbury, M. *Tetrahedron* **1980**, *36*, 3327–3359.
- (9) Ackermann, L.; Born, R.; Spatz, J. H.; Meyer, D. *Angew. Chem., Int. Ed.* **2005**, *44*, 7216–7219.
- (10) Hatakeyama, T.; Hashimoto, S.; Ishizuka, K.; Nakamura, M. *J. Am. Chem. Soc.* **2009**, *131*, 11949–11963.
- (11) Shirakawa, E.; Hayashi, Y.; Itoh, K.-i.; Watabe, R.; Uchiyama, N.; Konagaya, W.; Masui, S.; Hayashi, T. *Angew. Chem., Int. Ed.* **2012**, *51*, 218–221.
- (12) Doubina, N.; Stoddard, M.; Bronstein, H. A.; Jen, A. K. Y.; Luscombe, C. K. *Macromol. Chem. Phys.* **2009**, *210*, 1966–1972.
- (13) Ghosh, R.; Emge, T. J.; Krogh-Jespersen, K.; Goldman, A. S. *J. Am. Chem. Soc.* **2008**, *130*, 11317–11327.
- (14) Braga, A. A. C.; Ujaque, G.; Maseras, F. *Organometallics* **2006**, *25*, 3647–3658.
- (15) Dierkes, P.; van Leeuwen, W. N. M. P. *J. Chem. Soc., Dalton Trans.* **1999**, 1519–1530.
- (16) Amatore, C.; Broeker, G.; Jutand, A.; Khalil, F. *J. Am. Chem. Soc.* **1997**, *119*, 5176–5185.
- (17) Serra-Muns, A.; Jutand, A.; Moreno-Mañas, M.; Pleixats, R. *Organometallics* **2008**, *27*, 2421–2427.
- (18) Niksch, T.; Görls, H.; Weigand, W. *Eur. J. Inorg. Chem.* **2010**, 95–105.
- (19) Smeets, A.; Van den Bergh, K.; De Winter, J.; Gerbaux, P.; Verbiest, T.; Koeckelberghs, G. *Macromolecules* **2009**, *42*, 7638–7641.
- (20) Kiriy, A.; Senkovskyy, V.; Sommer, M. *Macromol. Rapid Commun.* **2011**, *32*, 1503–1517.
- (21) Iovu, M. C.; Sheina, E. E.; Gil, R. R.; McCullough, R. D. *Macromolecules* **2005**, *38*, 8649–8656.
- (22) Miyakoshi, R.; Yokoyama, A.; Yokozawa, T. *J. Am. Chem. Soc.* **2005**, *127*, 17542–17547.
- (23) Yoshikai, N.; Matsuda, H.; Nakamura, E. *J. Am. Chem. Soc.* **2008**, *130*, 15258–15259.
- (24) Komber, H.; Senkovskyy, V.; Tkachov, R.; Johnson, K.; Kiriy, A.; Huck, W. T. S.; Sommer, M. *Macromolecules* **2011**, *44*, 9164–9172.
- (25) Achord, B. C.; Rawlins, J. W. *Macromolecules* **2009**, *42*, 8634–8639.
- (26) Liu, J.; Loewe, R. S.; McCullough, R. D. *Macromolecules* **1999**, *32*, 5777–5785.

- (27) Miyakoshi, R.; Shimono, K.; Yokoyama, A.; Yokozawa, T. *J. Am. Chem. Soc.* **2006**, *128*, 16012–16013.
- (28) Marshall, N.; Sontag, S. K.; Locklin, J. *Macromolecules* **2010**, *43*, 2137–2144.
- (29) Lee, S. R.; Bryan, Z. J.; Wagner, A. M.; McNeil, A. J. *Chem. Sci.* **2012**, *3*, 1562–1566.
- (30) Krasovskiy, A.; Knochel, P. *Angew. Chem., Int. Ed.* **2004**, *43*, 3333–3336.
- (31) Shao, Y.; Molnar, L. F.; Jung, Y.; Kussmann, J.; Ochsenfeld, C.; Brown, S. T.; Gilbert, A. T. B.; Slipchenko, L. V.; Levchenko, S. V.; O'Neill, D. P.; DiStasio, R. A., Jr.; Lochan, R. C.; Wang, T.; Beran, G. J. O.; Besley, N. A.; Herbert, J. M.; Yeh Lin, C.; Van Voorhis, T.; Hung Chien, S.; Sodt, A.; Steele, R. P.; Rassolov, V. A.; Maslen, P. E.; Korambath, P. P.; Adamson, R. D.; Austin, B.; Baker, J.; Byrd, E. F. C.; Dachsel, H.; Doerksen, R. J.; Dreuw, A.; Dunietz, B. D.; Dutoi, A. D.; Furlani, T. R.; Gwaltney, S. R.; Heyden, A.; Hirata, S.; Hsu, C.-P.; Kedziora, G.; Khalliulin, R. Z.; Klunzinger, P.; Lee, A. M.; Lee, M. S.; Liang, W.; Lotan, I.; Nair, N.; Peters, B.; Proynov, E. I.; Pieniazek, P. A.; Rhee, Y. M.; Ritchie, J.; Rosta, E.; Sherrill, C. D.; Simmonett, A. C.; Subotnik, J. E.; Woodcock, H. L., III; Zhang, W.; Bell, A. T.; Chakraborty, A. K.; Chipman, D. M.; Keil, F. J.; Warshel, A.; Hehre, W. J.; Schaefer, H. F., III; Kong, J.; Krylov, A. I.; Gill, P. M. W.; Head-Gordon, M. *Phys. Chem. Chem. Phys.* **2006**, *8*, 3172–3191.
- (32) Lee, C.; Yang, W.; Parr, R. G. *Phys. Rev. B* **1988**, *37*, 785–789.
- (33) Becke, A. D. *J. Chem. Phys.* **1993**, *98*, 5648–5652.
- (34) Xu, Z.-F.; Xie, Y.; Feng, W.-L.; Schaefer, H. F. *J. Phys. Chem. A* **2003**, *107*, 2716–2729.
- (35) Niu, S.; Hall, M. B. *Chem. Rev.* **2000**, *100*, 353–406.
- (36) Rosana, A.; Faza, O. N.; Lopez, C. S.; de Lera, A. R. *Org. Lett.* **2006**, *8*, 35–38.
- (37) Napolitano, E.; Farina, V.; Persico, M. *Organometallics* **2003**, *22*, 4030–4037.
- (38) Zhao, Y.; Truhlar, D. *Theor. Chem. Acta* **2008**, *120*, 215–241.
- (39) Adamo, C.; Barone, V. *J. Chem. Phys.* **1998**, *110*, 6158–6170.
- (40) Purvis, G. D.; Bartlett, J. J. *J. Chem. Phys.* **1982**, *76*, 1910–1918.
- (41) Dunning, T. H. *J. Chem. Phys.* **1970**, *53*, 2823–2834.
- (42) Huzinaga, S. *J. Chem. Phys.* **1965**, *42*, 1293–1303.
- (43) Bergner, A.; Dolg, M.; Kuchle, W.; Stoll, H.; Preuss, H. *Mol. Phys.* **1993**, *80*, 1431–1441.
- (44) Hood, D. M.; Pitzer, R. M.; Schaefer, H. F. *J. Chem. Phys.* **1979**, *71*, 705–713.
- (45) Wachters, A. J. H. *J. Chem. Phys.* **1970**, *52*, 1033–1037.
- (46) Korenaga, T.; Abe, K.; Ko, A.; Maenishi, R.; Sakai, T. *Organometallics* **2010**, *29*, 4025–4035.